Stationary mixed-polarization spatial solitons and their stability in semiconductor waveguides

D. C. Hutchings and J. M. Arnold
Department of Electronics and Electrical Engineering, University of Glasgow, Glasgow G12 8QQ, United Kingdom

D. F. Parker
Department of Mathematics and Statistics, University of Edinburgh, Edinburgh EH9 3JZ, United Kingdom

(Received 1 May 1998)

Coupled nonlinear Schrödinger equations are used to describe propagation in the presence of an anisotropic Kerr nonlinearity in the most common semiconductor waveguide configuration. Stationary soliton solutions are identified analytically for the single-polarization case and numerically for the mixed-polarization case. The stability of these stationary solutions is assessed by using a linear stability analysis. Analytic forms for the bifurcation points are given, where the single-polarization state becomes unstable and the mixed-polarization state emerges. A new form of polarization instability is also identified where the ''fast'' mode soliton becomes unstable to antisymmetric perturbations at low power. Numerical studies are used to confirm the linear stability analysis results. [S1063-651X(98)02411-8]

PACS number(s): 42.65.Tg, 42.70.Nq, 42.65.Sf, 42.82.Et

I. INTRODUCTION

There is currently a large research effort into the study of multicomponent solitons. The simplest variant of this is the interaction of two orthogonal polarization components. The system for mixed-polarization solitons studied most extensively, both experimentally and theoretically, is temporal solitons in an optical fiber [1–4]. Semiconductor slab waveguides (in particular, $Al_xGa_{1-x}As$ at ~ 1.5 μm) have proved to be a useful medium for studying spatial solitons and their dynamics [5,6]. Although in both of these systems the nonlinearity is of Kerr type, the assumptions of isotropic nonlinearity and of Kleinmann symmetry, commonly made in the case of silica, do not extend to semiconductors.

Studies of optical propagation in anisotropic cubic media initially only considered propagation parallel to a crystal axis giving fourfold rotational symmetry [7,8]. This geometry with the added assumption of Kleinmann symmetry has also received some attention in relation to spatial solitons using an average profile approach [9] and a linear stability analysis [10]. The complete form of the coupled propagation equations for an anisotropic cubic nonlinear refractive index has been developed recently [11]. Plane-wave polarization dynamics and initial finite-beam numerical studies have been considered [12]. Qualitative agreement has been demonstrated with observed polarization dynamics in $Al_xGa_{1-x}As$ waveguides [6]. With the inclusion of diffraction, the equations of motion are nonintegrable and in general mixed-polarization solutions can only be obtained numerically. In the present paper the stationary soliton solutions are studied for the standard geometry of semiconductor waveguides. In particular, the mixed-polarization stationary solutions are obtained numerically; linear stability analysis is performed analytically on single-polarization solitons and numerically in the general case.

II. COUPLED NONLINEAR SCHRÖDINGER EQUATIONS

The usual orientation for a semiconductor waveguide on a GaAs substrate is that the growth direction is parallel to a crystal axis [001]. Since the cleavage planes are [110] and equivalent, weakly guiding waveguides have the TE polarization parallel to [110] and TM polarization parallel to [001]. In anisotropic cubic media the general propagation equations are quite complex, with six nonlinear terms for each polarization component [11]. However, the higher degree of symmetry for this particular orientation results in some simplification of the propagation equations. The conventional approach of factoring out the single-moded envelope in the vertical direction has been employed, leading to

$$\begin{aligned} i\frac{\partial u}{\partial z}+\frac{\partial^2 u}{\partial x^2}-\gamma u+\left[\left(1-\frac{\sigma}{2}\right)uu^*+\left(1-\delta-\frac{\sigma}{2}\right)vv^*\right]u \\ +\left(\delta-\frac{\sigma}{2}\right)u^*v^2=0, \\ i\frac{\partial v}{\partial z}+\frac{\partial^2 v}{\partial x^2}+\gamma v+\left[\left(1-\delta-\frac{\sigma}{2}\right)uu^*+vv^*\right]v \\ +\left(\delta-\frac{\sigma}{2}\right)u^2v^*=0, \end{aligned} \tag{1}$$

where u and v are the scaled electric field amplitudes for the TE and TM components, respectively, such that the irradiance is $I_u=2n_0|u|^2/n_2^L[001]$ and $n_2^L[001]$ is the nonlinear refractive index for light linearly polarized parallel to a crystal axis (e.g., TM mode). All quantities in Eqs. (1) have been scaled to be dimensionless; the transverse and longitudinal coordinates have been scaled to the optical wavelength, $2kx\rightarrow x$ and $2kz\rightarrow z$. The parameter $\gamma=(k_{TM}-k_{TE})/4k$ is proportional to the (structurally induced) birefringence. The polarization dependence is introduced through the dimensionless parameters: σ is the nonlinear refractive anisotropy parameter and δ the nonlinear birefringence parameter [13,14]. For an isotropic medium with Kleinmann symmetry these material parameters take the values $\sigma=0$ and $\delta=1/3$, but in $Al_{0.18}Ga_{0.82}As$ at the half-band-gap measurements in-

dicate $\sigma=-0.54$ and $\delta=0.18$ [15]. This large degree of anisotropy for nonlinear refraction is also predicted from band-structure calculations [13]. Note that the anisotropy leads to an asymmetry in the self-phase-modulation terms for the two polarization components for this orientation and hence is substantially different from that studied in Refs. [9,10] (which also have one fewer material parameter, as Kleinmann symmetry is assumed).

III. REVIEW OF PLANE-WAVE POLARIZATION DYNAMICS

The plane-wave polarization evolution described by Eq. (1) neglecting the x derivatives has received some attention. An elegant method of solution is to consider the Hamiltonian of the problem and then the polarization evolution trajectories correspond to contours of the constant Hamiltonian (also keeping total power constant). This can be formulated in terms of field amplitudes [11] or in terms of the Stokes polarization parameters [12],

$$\begin{aligned} s_0&=|u|^2+|v|^2,\\ s_1&=|u|^2-|v|^2,\\ s_2&=u^*v+uv^*,\\ s_3&=-i(u^*v-uv^*). \end{aligned} \tag{2}$$

The Stokes parameters allow the trajectories to be illustrated on the Poincaré sphere.

In order to understand the polarization dynamics, it is instructive to examine stationary solutions and their dynamics. In the presence of birefringence, at low optical power levels the plane-wave stationary solutions correspond to linear polarizations parallel (TM) and perpendicular (TE) to the optic axis ([001]). As the power (nonlinear phase shift) increases, there is a threshold at which there is a bifurcation of the singly polarized stationary solutions. For the ''fast'' mode (smaller propagation constant) this is into two elliptically polarized stationary solutions aligned with the optic axis. This bifurcation has previously been recognized from the study of temporal solitons in a birefringent optical fiber [2,7]. In anisotropic systems, however, there is an additional bifurcation of the plane-wave stationary solution for the ''slow'' mode (larger propagation constant) into two linearly polarized states. An example of this is demonstrated in the polarization evolution trajectories on the Poincaré sphere in Fig. 1. These plane-wave bifurcation points can be specified analytically [12]. Using the formalism of this paper they are given by

$$\begin{aligned} s_0&=2\gamma/(2\delta-\sigma/2), \quad \text{TE}, \quad \gamma>0\\ s_0&=4\gamma/\sigma, \quad \text{TE}, \quad \gamma<0\\ s_0&=-2\gamma/\sigma, \quad \text{TM}, \quad \gamma>0\\ s_0&=-\gamma/\delta, \quad \text{TM}, \quad \gamma<0. \end{aligned} \tag{3}$$

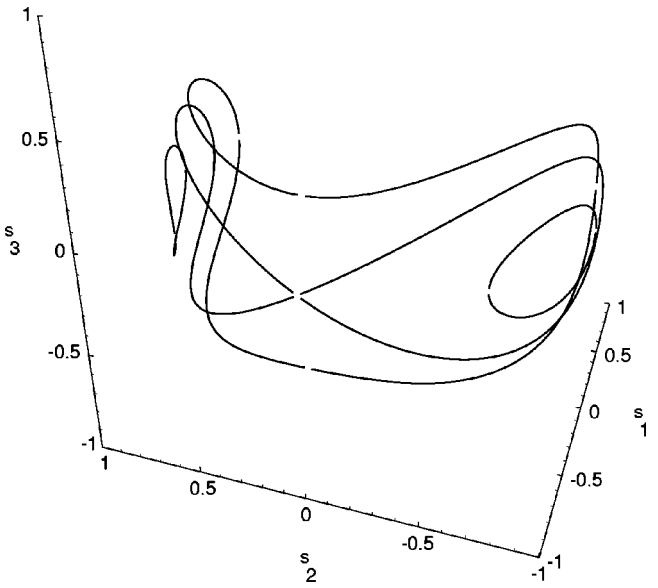

FIG. 1. Polarization evolution trajectories for a plane-wave in $Al_xGa_{1-x}As$ with the usual orientation in terms of the Stokes parameters. The ratio of birefringence to nonlinearity $\Delta k/k_{NL}$ is taken to be 0.3 here, illustrating the bifurcation in the TM-only polarized stationary solution.

IV. SOLITON STATIONARY SOLUTIONS

Among the stationary solutions to Eq. (1) are single-polarization solitons. This can be seen by substituting $u=0$ (or alternatively $v=0$) in Eq. (1) to obtain the usual scalar nonlinear Schrödinger equation (NLSE) in the TM (or TE) polarization component only. The lowest order soliton in this case takes the usual form,

$$v=\frac{\sqrt{2}}{a}\operatorname{sech}\left(\frac{x}{a}\right)\exp\left[i\left(\frac{1}{a^2}+\gamma\right)z\right]. \tag{4}$$

For the specific case of zero birefringence ($\gamma=0$) there are additional uniform polarization stationary solutions obtained by reducing the coupled NLSE's to a single equation. In the plane-wave case there are stationary polarization solutions: (1) linearly polarized parallel to [111], given in terms of the Stokes parameters as $s_1=s_0/3$ and $s_3=0$, and (2) elliptically polarized states aligned with the optic axis such that $s_1=s_0\sigma/(8\delta-\sigma)$ and $s_2=0$. Assuming a solution with a uniform polarization state corresponding to one of these plane-wave solutions again reduces Eq. (1) to the scalar form and the nonlinear coefficient is scaled appropriately. For example, in the [111]-linear polarization case we take $u=\sqrt{2/3}w$ and $v=\sqrt{1/3}w$ and the scalar NLSE has the nonlinear refractive coefficient for this polarization, $n_2^L[111]=(1-2\sigma/3)n_2^L[001]$.

In order to proceed with the general case of a nonzero birefringence ($\gamma\neq 0$) we first refer back to the plane-wave case. The two classes of mixed-mode stationary solution correspond to (1) linear polarization (at some angle to the optic axis), which in terms of the Stokes parameters corresponds to the ''equator'' on the Poincaré sphere, $s_3=0$, or (2) elliptical polarization aligned with the optic axis corresponding to the ''meridian'' of the Poincaré sphere, $s_2=0$. In the former case the components u and v are in phase, and in the latter

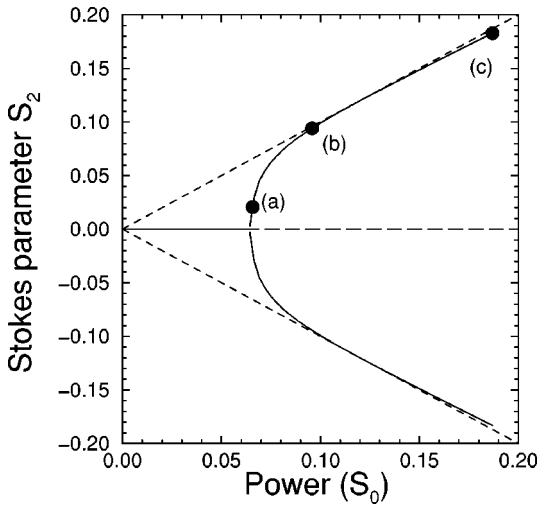

FIG. 2. Plot showing the integrated Stokes parameters for the stationary soliton solutions (solid line) for the $Al_xGa_{1-x}As$ example taking $\gamma=10^{-4}$. The bifurcation of the TM-only polarized solution is demonstrated here. The long-dashed line indicates the unstable continuation of the TM-only polarized soliton stationary solution. The short dashed lines indicate the maximum/minimum values of S_2, i.e., $S_2/S_0=\pm 1$. The points (a)–(c) refer to the calculated profiles in Fig. 3.

case exactly in quadrature. Therefore in the spatial soliton case we will consider the two classes of stationary solution: (1) linearly polarized, $u(z,x)=U(x)\exp(i\Omega z)$, $v(z,x)=V(x)\exp(i\Omega z)$, which reduces Eq. (1) to the pair of ODE's:

$$\frac{d^2U}{dx^2}-(\Omega+\gamma)U+\left[\left(1-\frac{\sigma}{2}\right)U^2+(1-\sigma)V^2\right]U=0,$$
$$\frac{d^2V}{dx^2}-(\Omega-\gamma)V+[(1-\sigma)U^2+V^2]V=0; \tag{5}$$

(2) elliptically polarized $u(z,x)=U(x)\exp(i\Omega z)$, $v(z,x)=iV(x)\exp(i\Omega z)$ giving the ODE's

$$\frac{d^2U}{dx^2}-(\Omega+\gamma)U+\left[\left(1-\frac{\sigma}{2}\right)U^2+(1-2\delta)V^2\right]U=0,$$
$$\frac{d^2V}{dx^2}-(\Omega-\gamma)V+[(1-2\delta)U^2+V^2]V=0. \tag{6}$$

$U(x)$ and $V(x)$ are real functions in both cases, and Ω is a parameter that will ultimately be related to power.

The method of seeking solutions $U(x)$ and $V(x)$ is as follows. Bound solutions have the asymptotic form at large $|x|$ found by ignoring the nonlinear terms in Eq. (5) or (6), thus giving

$$U(x)\sim U_0\exp-(\sqrt{\Omega+\gamma})|x|,$$
$$V(x)\sim V_0\exp-(\sqrt{\Omega-\gamma})|x|. \tag{7}$$

These asymptotic forms and their derivatives are used as initial conditions for numerical integration of the full ODE's towards $x=0$, using the Runge-Kutta method. Symmetry arguments dictate that $U(x)$ and $V(x)$ must be even or odd functions; the fundamental soliton falls into the category in which both functions are even. Hence we look for zeros of both dU/dx and dV/dx at $x=0$, by minimizing $(dU/dx)^2+(dV/dx)^2$ as a function of the initial parameters (U_0,V_0). In principle, this approach could be extended to search for even/odd or odd/odd solutions, but these higher-order solutions could not be located numerically and it is known that solutions of this form tend to be unstable [4].

As an example, we shall look in more detail at the linearly polarized mixed-mode stationary soliton given by the solution of Eq. (5) with positive $\gamma=10^{-4}$. To illustrate the locus of solutions, we make use of the integrated Stokes parameters,

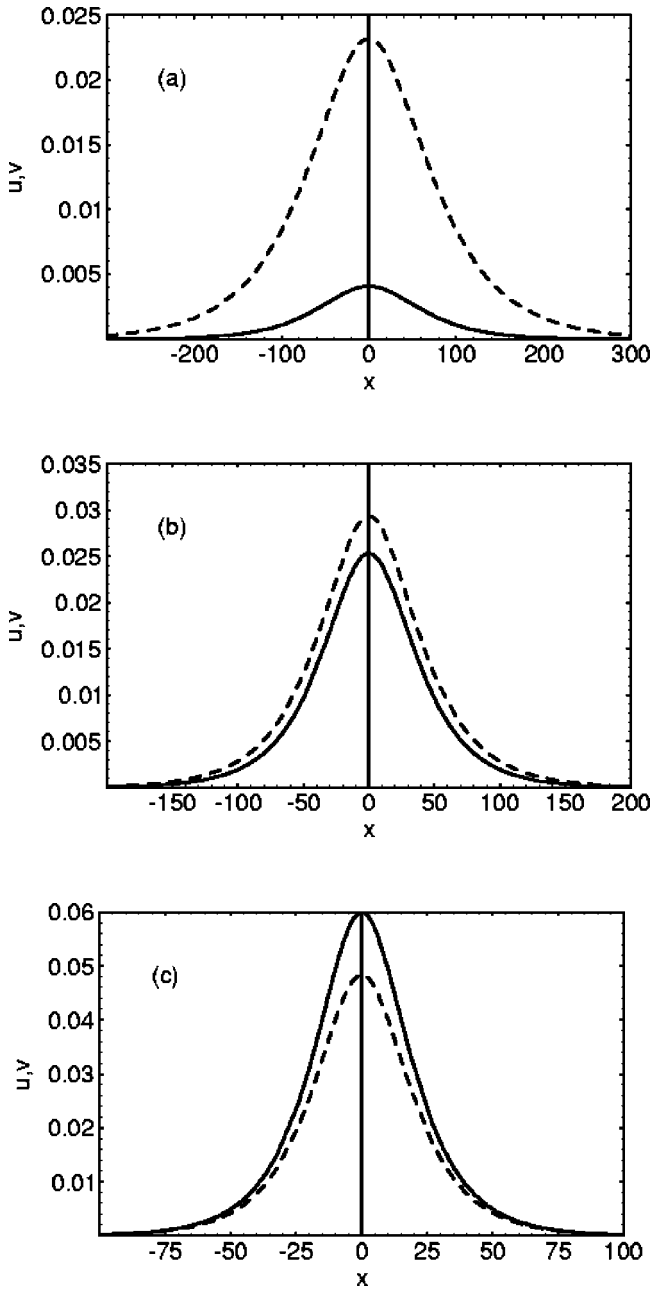

FIG. 3. Calculated amplitude profiles for the mixed-mode linearly polarized soliton stationary solutions. (a)–(c) correspond to the points indicated in Fig. 2. The solid line is the TE-polarized component and dashed line is the TM-polarized component.

$$S_j = \int_{-\infty}^{\infty} s_j(x)\,dx \quad . \tag{8}$$

In particular, the total optical power is proportional to S_0. In Fig. 2 the mixed-mode stationary solution is shown plotted as S_2 against S_0. In addition, the TM-only polarized stationary soliton is shown as the line $S_2=0$. The short-dashed lines indicate that all solutions must lie in the region $|S_2| \leqslant S_0$. It can be seen that the pair of mixed-mode stationary solutions only exists at optical powers above a certain threshold. The points indicated on the mixed-mode stationary solutions correspond to the profiles shown in Fig. 3(a)–3(c). Note that both components are bell-shaped curves but of different widths, giving a polarization state that varies across the soliton profile. As the total optical power varies, there is a considerable variation in the relative power in each mode and in the width of each component.

V. LINEARIZED FORM

One conventional method for analyzing the stability of the stationary solutions is to examine the dynamics of a small perturbation from this solution [1]. Substituting in Eq. (1) $u=[U_0(x)+\epsilon_U(z,x)]\exp(i\Omega z)$ and $v=[V_0(x)+\epsilon_V(z,x)]\exp(i\Omega z)$ where U_0 and V_0 are known solutions to Eq. (5) and ϵ_U and ϵ_V are the small perturbations (so only terms linear in $\epsilon_{U,V}$ need be retained) provides

$$\begin{aligned} i\frac{\partial \epsilon_U}{\partial z} + \frac{\partial^2 \epsilon_U}{\partial x^2} - (\Omega+\gamma)\epsilon_U + \left(1-\frac{\sigma}{2}\right)(2\epsilon_U+\epsilon_U^*)U_0^2 \\ + \left[\left(1-\delta-\frac{\sigma}{2}\right)(\epsilon_V+\epsilon_V^*) + 2\left(\delta-\frac{\sigma}{2}\right)\epsilon_V\right]U_0V_0 \\ + \left[\left(1-\delta-\frac{\sigma}{2}\right)\epsilon_U + \left(\delta-\frac{\sigma}{2}\right)\epsilon_U^*\right]V_0^2 = 0, \end{aligned}$$

$$\begin{aligned} i\frac{\partial \epsilon_V}{\partial z} + \frac{\partial^2 \epsilon_V}{\partial x^2} - (\Omega-\gamma)\epsilon_V + \left[\left(1-\delta-\frac{\sigma}{2}\right)\epsilon_V \right. \\ \left. + \left(\delta-\frac{\sigma}{2}\right)\epsilon_V^*\right]U_0^2 + \left[\left(1-\delta-\frac{\sigma}{2}\right)(\epsilon_U+\epsilon_U^*) \right. \\ \left. + 2\left(\delta-\frac{\sigma}{2}\right)\epsilon_U\right]U_0V_0 + (2\epsilon_V+\epsilon_V^*)V_0^2 = 0. \end{aligned} \tag{9}$$

Writing the perturbations ϵ_U, ϵ_V as oscillatory functions, e.g.,

$$\begin{aligned} \epsilon_j = \tfrac{1}{2}[X_j(x)+Y_j(x)]\exp(i\lambda z) \\ + \tfrac{1}{2}[X_j(x)-Y_j(x)]^*\exp(-i\lambda^* z) \quad (\text{for } j=U,V), \end{aligned} \tag{10}$$

where X_j and Y_j refer to the in-phase and in-quadrature components of the perturbations ϵ_j, collecting terms proportional to $\exp(i\lambda z)$ and $\exp(-i\lambda^* z)$, and rearranging, we obtain

$$\begin{aligned} L_1\mathbf{Y} &= \lambda\mathbf{X}, \\ L_2\mathbf{X} &= \lambda\mathbf{Y}, \end{aligned} \tag{11}$$

where the vector $\mathbf{X}=\binom{X_u}{X_v}$. The operators L_1 and L_2 are defined by

$$L_1 = \begin{pmatrix} \dfrac{d^2}{dx^2} - (\Omega+\gamma) + \left(1-\dfrac{\sigma}{2}\right)U_0^2 + (1-2\delta)V_0^2 & 2\left(\delta-\dfrac{\sigma}{2}\right)U_0V_0 \\ 2\left(\delta-\dfrac{\sigma}{2}\right)U_0V_0 & \dfrac{d^2}{dx^2} - (\Omega-\gamma) + (1-2\delta)U_0^2 + V_0^2 \end{pmatrix}, \tag{12}$$

$$L_2 = \begin{pmatrix} \dfrac{d^2}{dx^2} - (\Omega+\gamma) + 3\left(1-\dfrac{\sigma}{2}\right)U_0^2 + (1-\sigma)V_0^2 & 2(1-\sigma)U_0V_0 \\ 2(1-\sigma)U_0V_0 & \dfrac{d^2}{dx^2} - (\Omega-\gamma) + (1-\sigma)U_0^2 + 3V_0^2 \end{pmatrix}.$$

Since L_1 and L_2 are self-adjoint operators, Eqs. (11) indicate that λ^2 is real, i.e., the eigenvalue λ is either pure real, corresponding to a stable perturbation, or pure imaginary, corresponding to an exponentially growing, unstable perturbation. We note that this two-dimensional eigenvalue equation has a similar form to Ref. [10] although the initial coupled differential equations are different.

The linear stability analysis of the elliptically polarized solitons is very similar. The same form is obtained for the eigenvalue equation, Eq. (11), but the operators L_1 and L_2 are slightly modified as

$$L_1=\begin{pmatrix} \frac{d^2}{dx^2}-(\Omega+\gamma)+\left(1-\frac{\sigma}{2}\right)U_0^2+(1-\sigma)V_0^2 & -2\left(\delta-\frac{\sigma}{2}\right)U_0V_0 \\ -2\left(\delta-\frac{\sigma}{2}\right)U_0V_0 & \frac{d^2}{dx^2}-(\Omega-\gamma)+(1-\sigma)U_0^2+V_0^2 \end{pmatrix},$$

$$L_2=\begin{pmatrix} \frac{d^2}{dx^2}-(\Omega+\gamma)+3\left(1-\frac{\sigma}{2}\right)U_0^2+(1-2\delta)V_0^2 & 2(1-2\delta)U_0V_0 \\ 2(1-2\delta)U_0V_0 & \frac{d^2}{dx^2}-(\Omega-\gamma)+(1-2\delta)U_0^2+3V_0^2 \end{pmatrix}. \tag{13}$$

Now consider the specific case of a single-polarization soliton for which the analytic solution is available in Eq. (4). The off-diagonal terms in the operators L_1 and L_2 are zero, and therefore Eqs. (11) decouple into sets of equations separately describing each polarization component of the perturbation. As an example, we consider the stationary solution with only a TM-polarized component $U_0=0$; a similar analysis applies for the TE-only case. The stability eigenvalue equations for the same polarization component can be written as

$$\left[\frac{d^2}{dx^2}-(\Omega-\gamma)+V_0^2\right]Y_v=\lambda X_v,$$
$$\left[\frac{d^2}{dx^2}-(\Omega-\gamma)+3V_0^2\right]X_v=\lambda Y_v. \tag{14}$$

This form has been well studied for the scalar NLSE [16,17]. Solutions to these include the case $\lambda=0$, which gives marginal stability. For a bounded solution V_0, we get $Y_v\propto V_0$, which corresponds to a phase shift, and $X_v\propto dV_0/dx$, which corresponds to a position shift.

The stability eigenvalue equations for the opposite- (TE-) polarization component in the TM-only stationary solution are

$$\left[\frac{d^2}{dx^2}-(\Omega+\gamma)+(1-2\delta)V_0^2\right]Y_u=\lambda X_u,$$
$$\left[\frac{d^2}{dx^2}-(\Omega+\gamma)+(1-\sigma)V_0^2\right]X_u=\lambda Y_u. \tag{15}$$

Here we have used the linear-polarization stationary-solution form for the operators given in Eqs. (12), but the result for the polarization stability of the single-polarization soliton follows also for the alternate form.

Note that in these opposite-polarization eigenvalue equations (unlike the same-polarization case) a number of nonlinear refractive parameters such as σ and δ remain. Thus it is anticipated that as the soliton power changes, the eigenvalues of Eqs. (15) will vary. We are particularly interested in the threshold that marks the transition from a stable to an unstable perturbation. Since λ^2 is always real, this must occur at $\lambda=0$. On inserting this value into Eqs. (15) the two polarization components decouple. Taking the stationary solution for the TM-only component given by Eq. (4) and making the substitution $t=\tanh(x/a)$ then both of Eqs. (15) reduce to the defining ODE for associated Legendre functions [18]. The linearly independent solutions are $P_\nu^\mu(t)$ and $Q_\nu^\mu(t)$ or, alternatively, providing μ is not an integer, $P_\nu^{\pm\mu}(t)$, where

$$P_\nu^\mu(t)=\frac{1}{\Gamma(1-\mu)}\left(\frac{1+t}{1-t}\right)^{\mu/2}\times F\left(-\nu,\nu+1;1-\mu;\frac{1-t}{2}\right) \tag{16}$$

and $F(a,b;c;z)$ is the hypergeometric function. The order μ and degree ν of the associated Legendre functions are given by

$$\mu^2=1+2a^2\gamma,\quad \nu(\nu+1)=2(1-\sigma)\quad \text{for } X_u, \tag{17}$$

$$\mu^2=1+2a^2\gamma,\quad \nu(\nu+1)=2(1-2\delta)\quad \text{for } Y_u. \tag{18}$$

There are two roots $\nu_{1,2}$ in each case for the order ν, which are related by $\nu_2+1=-\nu_1$. The TE-only case can be similarly analyzed and also produces associated Legendre functions for the eigenfunctions with $\lambda=0$ but with the order and degree given by

$$\mu^2=1-2a^2\gamma,\quad \nu(\nu+1)=2\frac{(1-\sigma)}{\left(1-\frac{\sigma}{2}\right)}\quad \text{for } X_v, \tag{19}$$

$$\mu^2=1-2a^2\gamma,\quad \nu(\nu+1)=2\frac{(1-2\delta)}{\left(1-\frac{\sigma}{2}\right)}\quad \text{for } Y_v. \tag{20}$$

Here we are interested in eigenfunctions that are bounded, requiring $X(t),\ Y(t)\to 0$ as $t\to\pm 1$. At these limits the hypergeometric function takes the forms [18]

$$F(a,b;c;1)=\frac{\Gamma(c)\Gamma(c-a-b)}{\Gamma(c-a)\Gamma(c-b)},$$
$$F(a,b;c;0)=1. \tag{21}$$

Taking the positive square root (i.e., $\mu>0$), it can be seen from Eqs. (16) and (21) that $P_\nu^\mu(t)$ is singular at $t=1$. Therefore the eigenfunctions are restricted to the negative root $X(t)$, $Y(t)=CP_\nu^{-\mu}(t)$. Furthermore, to satisfy $\lim_{t\to-1}P_\nu^{-\mu}(t)=0$, the hypergeometric function must vanish as $t\to-1$, corresponding to a pole of one or other gamma function in the denominator of Eq. (21), $\Gamma(\mu-\nu)$ or $\Gamma(1+\mu+\nu)$. Therefore it is necessary that $(\mu-\nu)$ is zero or a negative integer for one of the possible values for the order ν. Typical values of the material parameters (e.g., half-band-gap nonlinearity in direct-gap semiconductors) are $-2<\sigma\leqslant 0$ and $0\leqslant\delta\leqslant 1/3$. These impose restrictions on the positive root for the degree ν: (1) for Eqs. (17) and (19), $1\leqslant\nu<2$, and (2) for Eqs. (18) and (20), $0<\nu\leqslant 1$. Hence, overall only the cases $\mu=\nu$ and $\mu=\nu-1$ need be considered here. These two cases correspond to a symmetric and antisymmetric eigenfunction, respectively.

Consider first the TM-only polarized stationary solution with the order and degree of the eigenfunction given by Eqs. (17) and (18). If the structural birefringence parameter γ is positive (indicating $n_{\mathrm{TM}}>n_{\mathrm{TE}}$), then $\mu>1$ and the only stability threshold that applies is $\mu=\nu$ (symmetric eigenfunction) using Eq. (17). The optical power in the soliton is proportional to a^{-1}, therefore with increasing power the parameter μ decreases towards unity according to Eq. (17). The threshold $\mu=\nu$ here is the soliton equivalent of the plane-wave bifurcation point [11,12], where the TM-only wave becomes unstable with the stationary solution bifurcating into two linearly polarized stationary solutions. For $\gamma<0$, Eq. (18) provides $\mu<1$, increasing with optical power. There is also a soliton stability threshold that corresponds to the previously investigated plane-wave bifurcation point (into elliptically polarized stationary solutions) given by $\mu=\nu$ (symmetric) and Eq. (18). However, taking the measured values for $Al_{0.18}Ga_{0.82}As$ [15], $\sigma=-0.54$ and $\delta=0.18$, the stability threshold condition $\mu=\nu-1$ (antisymmetric perturbation) with Eq. (17) is reached at lower optical power levels. Figure 4 shows the calculated eigenfunctions at these three stability thresholds.

Consideration of the TE-only case gives similar results. The plane-wave bifurcation into linearly polarized stationary solutions for $\gamma<0$ has its counterpart in the soliton case given by $\mu=\nu$ and Eq. (19). For $\gamma>0$ there is the equivalent of the plane-wave bifurcation into elliptically polarized stationary solutions but it is preceded by the antisymmetric stability threshold given by $\mu=\nu-1$ and Eq. (19), at least in the $Al_{0.18}Ga_{0.82}As$ example. Generalizing, the antisymmetric instability occurs in the *fast* mode (i.e., the mode with the lower propagation constant), the stationary solutions of which bifurcate into elliptically polarized solutions.

The general stability case can be considered numerically by making use of Evans' approach [19,20]. This is constructed in the following manner. First we consider the asymptotic form of the eigenvalue equation (11) obtained by ignoring the nonlinear contributions and setting U_0 and V_0 equal to zero. The two polarization components decouple, and decaying exponential solutions ($\propto\exp\mp\eta x$ for $x\to\pm\infty$, respectively) are obtained and $Y_i/X_i=\pm 1$. This gives a total of eight ''independent'' asymptotic solutions. Each of these asymptotic forms is used as the initial condition in an initial value problem (set of coupled linear ODE's), integrating in each case to the same point ($x=0$). Then a determinant, dependent on the value chosen for the eigenvalue λ, is constructed consisting of the numerically determined values of $(X_u, X_u', Y_u, Y_u', X_v, X_v', Y_v, Y_v')$ for each of the eight ''independent'' solutions. Now if a value is chosen for the eigenvalue λ that corresponds to a bound solution (tends to zero at both $x=\pm\infty$), then there will not be complete independence between solutions generated for positive and negative x and the determinant will be zero. Therefore, the eigenvalue problem reduces to one of finding the zeros of the determinant as a function of λ. For determining the stability it is sufficient to locate λ on the real or imaginary axis in this case.

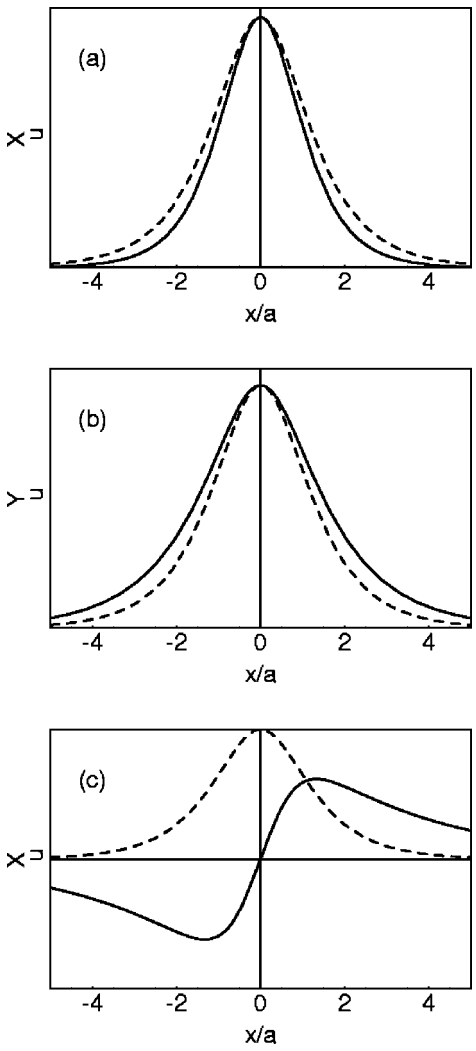

FIG. 4. The TE-polarized perturbation eigenfunctions at the threshold of instability for a TM-only polarized soliton calculated using the measured nonlinear refractive parameters for $Al_{0.18}Ga_{0.82}As$ at the half-band-gap. For comparison the sech envelope of the TM-polarized soliton is also shown (dashed). Transverse dimensions are given in terms of the soliton width a. (a) occurs for $n_{\mathrm{TM}}>n_{\mathrm{TE}}$, (b) is the symmetric and (c) the antisymmetric eigenfunctions, respectively, for $n_{\mathrm{TM}}<n_{\mathrm{TE}}$.

In the case of the ''slow'' optical mode (i.e., TM when $\gamma>0$ and TE when $\gamma<0$) it is found that for power levels below the bifurcation point, all the eigenvalues for the singly polarized soliton are real and therefore correspond to stable stationary states. At power levels above the bifurcation point

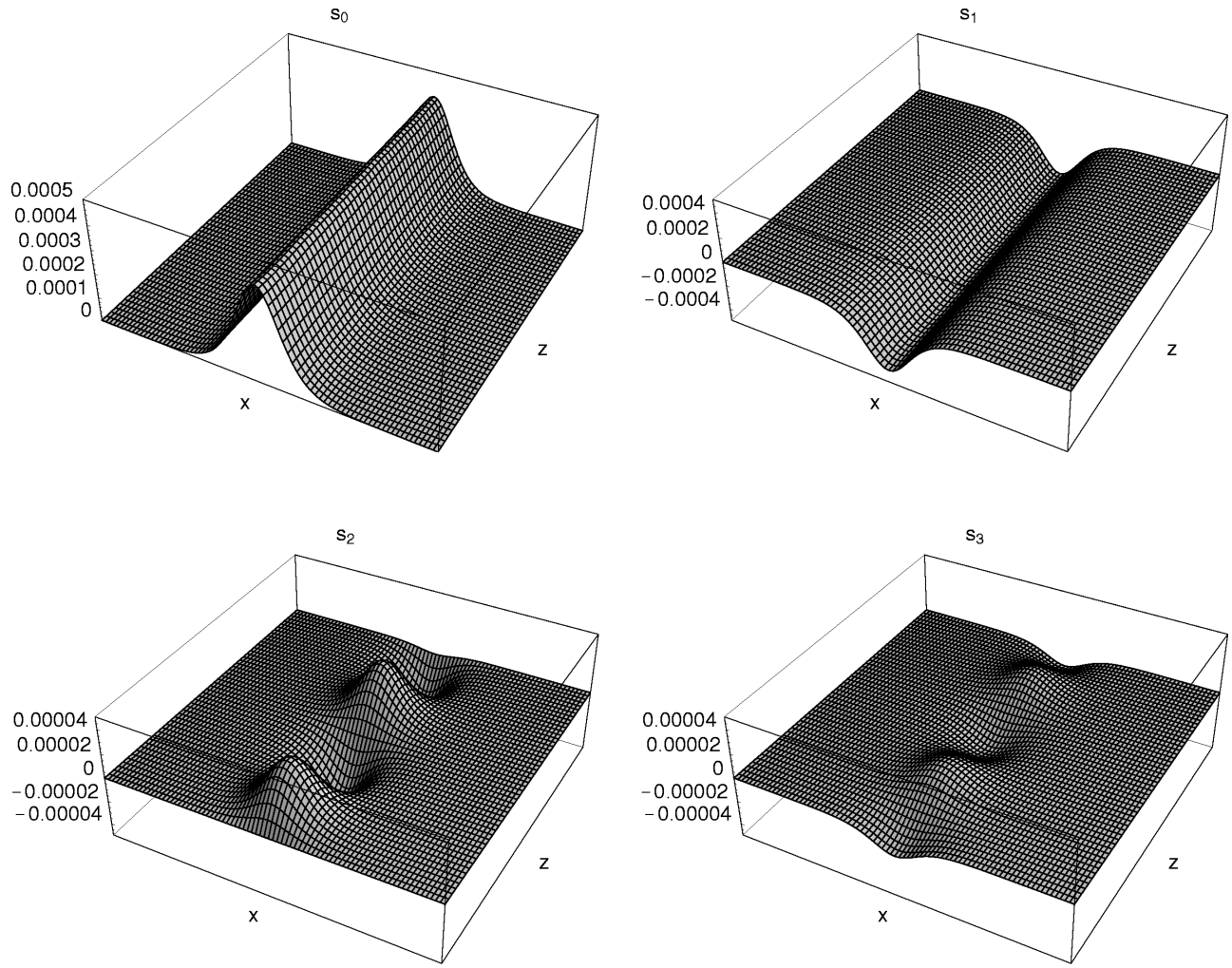

FIG. 5. Calculated evolution of the Stokes parameters defined in Eq. (2). The transverse coordinate x is shown over the range -400–400 (computational window -1000–1000) and the longitudinal coordinate z over the range 0–10^5. This example shows the stable symmetric perturbation (2% amplitude launched in TE polarization) of a TM-only polarized stationary soliton. Note that the vertical axes for s_2 and s_3 have been expanded by a factor of 10 in comparison to s_1.

a pair of eigenvalues become imaginary for the singly polarized soliton indicating instability to symmetric perturbations. Simultaneously, mixed-polarization stationary soliton solutions are allowed (linear polarization) that are found to have only real eigenvalues and hence are stable.

For the ''fast'' optical mode (i.e. TM when $\gamma<0$ and TE when $\gamma>0$) the behavior around the bifurcation point is similar to the previous case. At power levels just below the bifurcation, only the singly polarized stationary solutions exist, which have only real eigenvalues are hence are stable. Above the bifurcation point these develop a pair of imaginary eigenvalues but simultaneously a mixed-polarization stationary soliton (elliptically polarized) comes into existence with only real eigenvalues. However, at lower optical power levels there is the additional threshold corresponding to an antisymmetric perturbation. For the singly polarized stationary soliton it is found that imaginary eigenvalues appear at power levels *below* this threshold. Hence at low optical powers, the (singly polarized) ''fast'' mode soliton is unstable to antisymmetric perturbations, becomes stable at higher power levels, and becomes unstable to symmetric perturbations at yet higher power levels (bifurcation point).

VI. NUMERICAL STUDIES

A limitation of the linear stability analysis is that it provides useful information only when the perturbations are small. In a regime where the perturbation has initially exponential growth, this analysis is insufficient to follow the complete evolution. In such cases it is necessary to resort to numerical computation of the evolution of the optical envelope given by the coupled PDE's in Eq. (1). In Figs. 5–7 three case studies are shown. In each case all four Stokes parameters are plotted to demonstrate the polarization evolution. The initial conditions in each case are taken to be the TM-only polarized stationary soliton plus a TE-polarized perturbation with 2% of the amplitude (i.e., 0.04% power).

In Fig. 5 the initial conditions are such that the soliton is stable to a symmetric perturbation. This is confirmed numerically with the profiles $s_2(x)$ and $s_3(x)$ undergoing oscillations limited by the initial amplitude of $s_3(x)$ (note the vertical scale has been expanded to illustrate this), and $s_0(x)$ and $s_1(x)$ profiles are essentially constant during propagation. In Fig. 6 the initial optical power has been increased beyond the bifurcation value. Now, the growths of the pro-

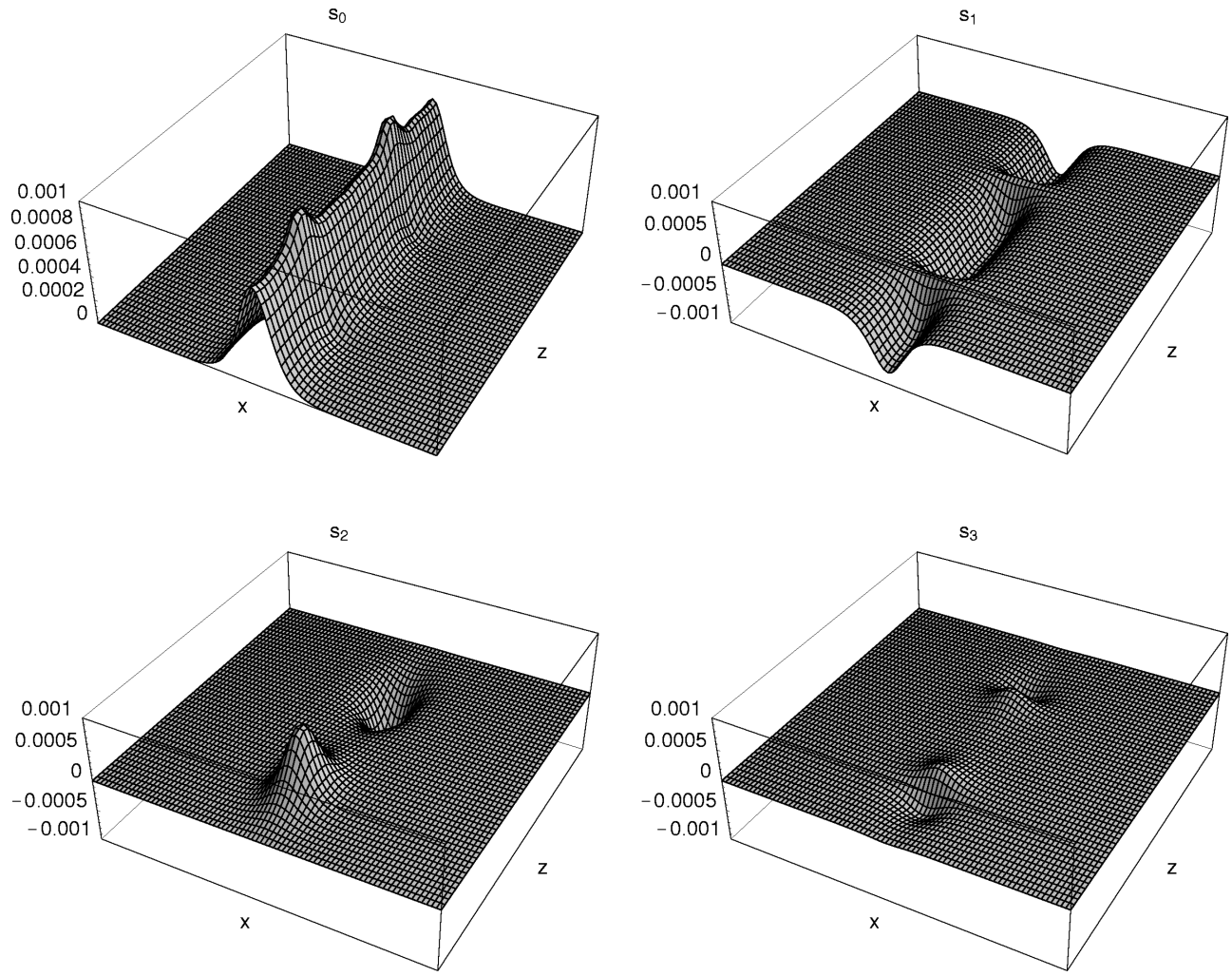

FIG. 6. Same as Fig. 5 except that the initial conditions correspond to the growth of the symmetric perturbation.

files $s_2(x)$ and $s_3(x)$ are not bounded by the initial amplitude of the perturbation. In addition $s_0(x)$ and $s_1(x)$ profiles also demonstrate a substantial modulation; in fact, in this example one extremum of the oscillation is approximately linearly polarized at 45° to the optic axis. However it appears in this example that there is not any significant radiation over the range investigated, with the ''soliton'' adjusting its width to compensate for the variation in nonlinearity with polarization vector. In Fig. 7 an antisymmetric perturbation is employed with the initial conditions corresponding to this perturbation being unstable. In this example the propagation range is extended by a factor of 3 to illustrate the dynamics. Again the profiles $s_2(x)$ and $s_3(x)$ initially demonstrate growth but in this case there is an eventual breakup of the soliton.

VII. CONCLUSIONS

This paper starts from the coupled PDE's describing propagation of two orthogonally polarized modes appropriate for the standard orientation of a semiconductor waveguide. It is not widely appreciated that the crystal symmetry in this system, together with the inapplicability of Kleinmann symmetry, leads to the form given in Eq. (1). In particular, there is an asymmetry between the two modes in the self-phase-modulation term. Here the stationary soliton solutions to Eq. (1) are investigated. It is noted that in the single polarization case, the coupled system reduces to the conventional nonlinear Schrödinger equation supporting fundamental sech envelope solitons. In addition there exist two families of mixed-polarization soliton corresponding to the phase difference between the two components being zero (linearly polarized) or $\pi/2$ (elliptically polarized aligned with the optic axis). The solutions to these are obtained numerically by solution of a pair of coupled ODE's. The only solutions obtained here are symmetric and bell shaped for both components with the relative widths and power dependent on the total power. Hence, although the type of polarization state is the same across the soliton, in the case of linear polarization, the orientation rotates, and in the case of elliptical polarization, the degree of ellipticity varies [as is common even for systems more symmetric than Eq. (1) [21]].

The polarization stability of the stationary soliton solutions is investigated using a linear stability analysis, which leads to an eigenvalue problem. Exact analytic solutions are known for single-polarization solitons that allow analytic results to be obtained at the instability threshold. The bifurcation points are found analytically from consideration of the boundary conditions of the associated Legendre function eigenfunction solutions. Numerical confirmation of the stability of the solutions on either side of this threshold is ob-

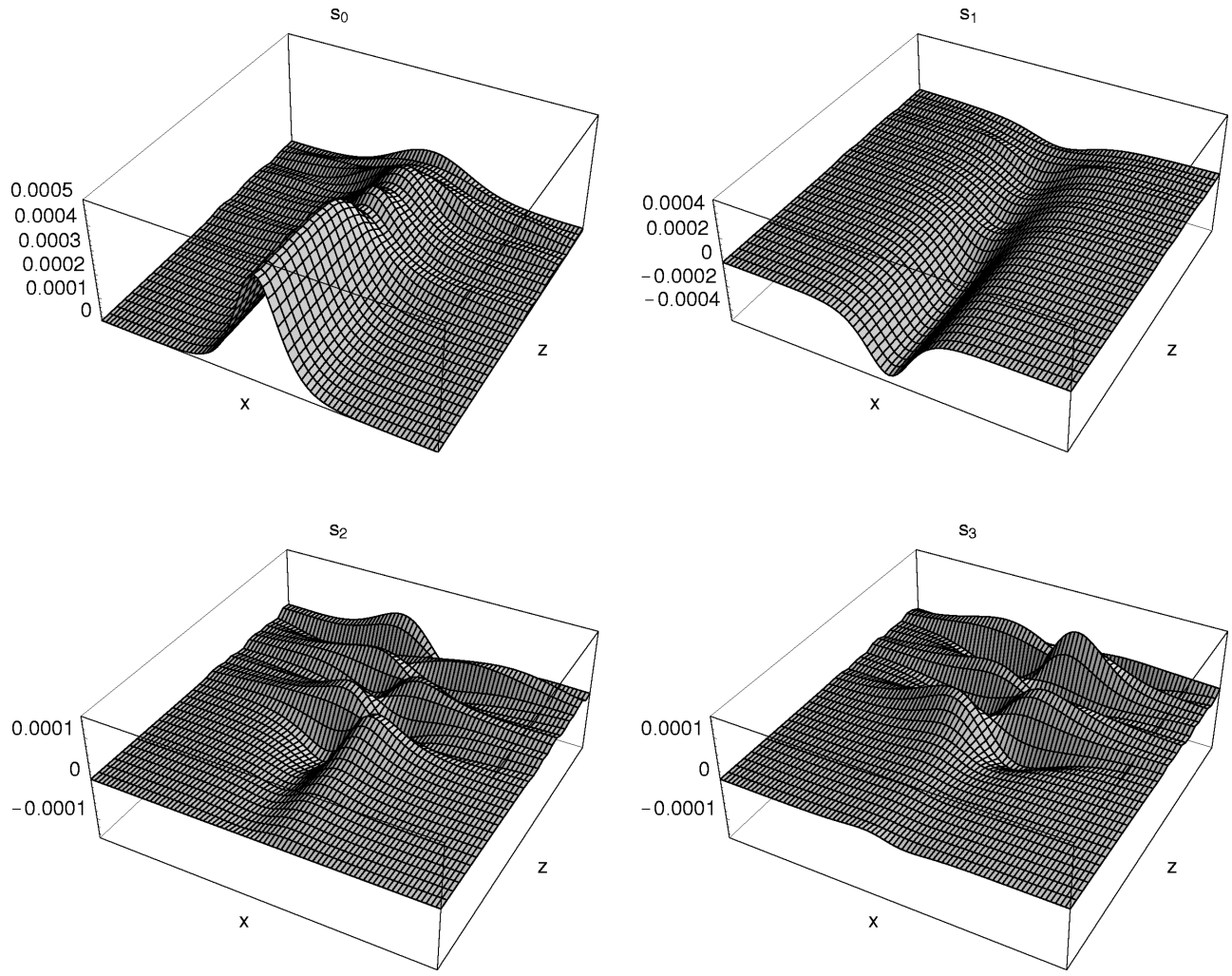

FIG. 7. Same as Fig. 5 except that the initial conditions correspond to the growth of the launched antisymmetric perturbation. The longitudinal coordinate has also been extended by a factor of 3 to show the eventual breakup of the soliton.

tained by an Evans function approach. As expected, the single-polarization stationary soliton solutions are stable below the bifurcation points but become unstable to a symmetric perturbation above this point, which coincides with the emergence of stable mixed-polarization stationary solutions. However, during this analysis a new form of instability was discovered that affects the ''fast'' polarization mode (normally TM). There is a threshold (given analytically) at lower power levels than the usual bifurcation. At power levels lower than this threshold the single-polarization soliton is unstable to an antisymmetric perturbation. Numerical solution of the coupled PDE's is also performed to confirm the results of the linear stability analysis.

Among other studies of multicomponent solitons is multiwavelength solitons coupled by four-wave-mixing [22]. It is interesting to note some commonalities of behavior. At the lowest optical power levels the single-component solitons are the only stable solution. As the power levels increase the stable solutions are replaced with multicomponent solitons (dual polarization in the present case, two- or three-wavelength in the case of Ref. [22]).

It is important to establish whether the polarization phenomena described in this paper are realizable with current experimental samples and apparatus. Typical spatial soliton widths in $Al_xGa_{1-x}As$ waveguides at a wavelength around 1.55 μm are of the order of 32 μm e^{-2} diameter [5]. In the dimensionless units used here this corresponds to a width of 860. The examples used in this paper are a factor of $\geqslant 2$ narrower, corresponding to a similar factor increase in optical power that is not unattainable. Similarly the largest value used for the longitudinal coordinate (3×10^5) corresponds to a physical length of 1.1 cm which is typical for $Al_xGa_{1-x}As$ waveguide samples. The structural birefringence of $\gamma = \Delta n/(4n) = \pm 10^{-4}$ taken here is typical for slab waveguides. By specifically designing weak-waveguiding structures this could easily be reduced by around an order of magnitude, although there are indications that stress-induced birefringence modifies the expected value [6]. Since the relevant factor in the polarization stability threshold is $a^2\gamma$, the soliton width at threshold is increased by a factor of ~ 2 with a similar reduction in optical power required.

ACKNOWLEDGMENTS

This work is supported by the Engineering and Physical Sciences Research Council. The authors thank J. S. Aitchison for valuable discussions.

[1] N. N. Akhmediev and A. Ankiewicz, *Solitons* (Chapman and Hall, London, 1997).
[2] D. N. Christodoulides and R. I. Joseph, Opt. Lett. **13**, 53 (1988).
[3] N. N. Akhmediev, A. V. Buryak, J. M. Soto-Crespo, and D. R. Andersen, J. Opt. Soc. Am. B **12**, 434 (1995).
[4] Y. Silberberg and Y. Barad, Opt. Lett. **20**, 246 (1995).
[5] J. S. Aitchison, K. Al-Hemyari, C. N. Ironside, R. S. Grant, and W. Sibbett, Electron. Lett. **20**, 1879 (1992).
[6] J. S. Aitchison, D. C. Hutchings, J. M. Arnold, J. U. Kang, G. I. Stegeman, E. Ostrovskaya, and N. Akhmediev, J. Opt. Soc. Am. B **14**, 3032 (1997).
[7] G. Gregori and S. Wabnitz, Phys. Rev. Lett. **56**, 600 (1986).
[8] M. V. Tratnik and J. E. Sipe, Phys. Rev. A **35**, 2965 (1987).
[9] E. A. Ostrovskaya, N. N. Akhmediev, G. I. Stegeman, J. U. Kang, and J. S. Aitchison, J. Opt. Soc. Am. B **14**, 880 (1997).
[10] Y. Chen, Phys. Rev. E **57**, 3542 (1998).
[11] D. C. Hutchings, J. S. Aitchison, and J. M. Arnold, J. Opt. Soc. Am. B **14**, 869 (1997).
[12] D. C. Hutchings, J. S. Aitchison, and J. M. Arnold, Opt. Quantum Electron. (to be published).
[13] D. C. Hutchings and B. S. Wherrett, Phys. Rev. B **52**, 8150 (1995).
[14] J. S. Aitchison, D. C. Hutchings, J. U. Kang, G. I. Stegeman, and A. Villeneuve, IEEE J. Quantum Electron. **33**, 341 (1997).
[15] D. C. Hutchings, J. S. Aitchison, B. S. Wherrett, G. T. Kennedy, and W. Sibbett, Opt. Lett. **20**, 991 (1995).
[16] G. Rowlands, J. Inst. Math. Appl. **13**, 367 (1974).
[17] J. M. Arnold, IMA J. Appl. Math. **52**, 123 (1994).
[18] *Handbook of Mathematical Functions*, edited by M. Abramowitz and I. A. Stegun (Dover, London, 1965).
[19] J. W. Evans, Indiana Univ. Math. J. **21**, 877 (1972); **22**, 75 (1972); **22**, 577 (1972); **24**, 1169 (1975).
[20] T. Kapitula, SIAM J. Math. Anal. (to be published).
[21] C. Sophocleous and D. F. Parker, Opt. Lett. **112**, 214 (1994).
[22] P. B. Lundquist, D. R. Andersen, and Y. S. Kivshar, Phys. Rev. E **57**, 3551 (1998).